PERGAMON

International Journal of Multiphase Flow 25 (1999) 1431–1456

International Journal of Multiphase Flow

www.elsevier.com/locate/ijmulflow

Fluidized bed in a confined volume

P. Vainshtein, M. Fichman, M. Shapiro*, L. Moldavsky, C. Gutfinger

Laboratory of Transport Processes in Porous Materials, Faculty of Mechanical Engineering, Technion-Israel Institute of Technology, Haifa 32000, Israel

Received 17 November 1998; received in revised form 10 May 1999

Dedicated to Professor Gad Hetsroni on the occasion of his 65th anniversary with kind wishes of good health and continuation of his creative and fruitful research work.

Abstract

Coarse solid elastic enough particles form a packed bed in a vertical cylinder confined from below and from above by permeable elastic plates. A gas is forced through the lower plate with a velocity exceeding the terminal (transport) velocity. Adjacent to the lower plate the particles are entrained and impact on the upper plate. As a result, fluidization regimes of still unreported types take place in the confined cylinder. These regimes are analyzed qualitatively by a theoretical model proposed here. This model describes the mean motions of the gas and particles. It includes the mass and momentum equations for the gas and particle phases and the equation of the kinetic energy of particle fluctuations. The system of equations is supplemented by constitutive equations for the averaged drag force, granular pressure, kinetic energy dissipation due to inelastic particle collisions, and energy generation. It is assumed that generation of the kinetic energy is caused by the lateral Magnus force due to particle rotation. Steady state solutions of the equations are obtained, which describe the fluidization regimes in a confined cylinder, namely disperse for a fluidized bed with increasing or decreasing volume fraction and for an inverted packed bed. Experiments are performed to show the existence of the disperse regime of fluidization. Stability of the disperse bed with respect to small perturbations is considered. It is shown that a disperse fluidized bed is unstable for sufficiently concentrated dispersions where the bulk modulus of elasticity of the granular phase is negative. The effect of vibrations of the upper plate upon fluidization regimes is also studied. Resonant frequencies are detected in the concentration region where the bulk modulus of elasticity is positive.

Keywords: Fluidized bed; Confined volume; Fluidization regimes

* Corresponding author. Tel.: +972-4832-4533; fax: +972-4829-3185.
E-mail address: mersm01@techunix.technion.ac.il (M. Shapiro)

0301-9322/99/$ - see front matter
PII: S0301-9322(99)00063-4

1. Introduction

Fluidization is an operation by which an assemblage of solid particles are transformed into a fluid-like state through contact with a flowing gas or liquid. Fluidized beds have considerable advantages for material processing and are used in numerous important industrial applications (Kuini and Levenspiel, 1991).

One of the research goals of fluidization is the delineation of the various gas–solid fluidization regimes and transitions between them. A fluid flowing slowly upward through a bed of solid particles merely percolates through the void spaces between the particles. This is a packed bed flow regime. With increasing flow rate, a stage is reached, when the particles are just suspended in the upward flowing gas or liquid. At this point the frictional force between particle and fluid counterbalances the particle weight, so that the pressure drop through any section of the bed is equal to the weight of the particles and fluid in that section. This state is referred to as minimum fluidization.

In gas–solid systems, when the flow rate exceeds that of minimum fluidization, large instabilities, namely bubbling and channeling, are observed, leading to a bubbling fluidized bed. As the gas velocity is further raised, the heterogeneous character of the bed gradually changes, giving way to increasing uniformity, culminating in the state in which no large discrete bubbles or voids are present. This regime prevails with the gas flow rate increasing up to the so-called terminal (or transport) velocity (Kuini and Levenspiel, 1991). As the terminal velocity is approached, there is a sharp increase in the rate of particle carryover. In the absence of solids recycling, the bed would empty in short order. Solids can be fed to the bottom of the column. Then, the fully entrained transport flow appears where the concentration of the resulting suspension depends on both the velocity of the gas and the feeding solid flow rate. Such a circulating bed is on the average almost homogeneous. If the particles are fed into the column bottom, e.g. via external cyclones and a standpipe, then it is possible to maintain in the column a relatively large solid concentration typical to the fast bed condition (Yerushalmi and Cancurt, 1979; Lim et al., 1995).

In this paper, we study new fluidization regimes when the terminal velocity is exceeded, possibly significantly, and the particles are contained within a volume confined from above by a permeable elastic plate. Sufficiently, elastic particles bounce off the upper plate. We will show that under certain conditions subsequent interparticle collisions bring about disperse fluidization in the confined cylinder. Otherwise, inelastic particles form an inverted packed bed (plug) adjacent to the upper plate. In this case, vibrations of the upper plate can be applied to bring the bed to a vibrofluidized state (Goldshtein et al., 1995). One could then consider combined vibro- and gas-fluidization of solid particles in a confined volume. One obvious advantage of such a system is that fluidization can, generally, proceed up to very high gas flowrates, resulting in very high relative gas-particle velocities. This can yield efficient heat and mass transfer between the gas and the particles, which is beneficial in many industrial fluidization operations. Note that in a confined fluidized bed the relative velocities can be much higher than those prevailing in a fast fluidized bed (Yerushalmi and Cancurt, 1979; Lim et al., 1995) where they are limited by the mean particle settling velocity in a homogenous fluidized bed, which is less than the terminal velocity.

This paper presents a theoretical model of disperse fluidization in a confined volume. Towards this goal, we review and modify existing models of other fluidization regimes.

There is extensive literature devoted to investigations of different aspects of the fluidization process, including works on fundamentals of fluidization, namely, minimum fluidizing velocity, terminal velocity, and pressure drop in a fluidized bed. For a thorough discussion of these works, the reader is referred to the book of Kuini and Levenspiel (1991) and the survey of Glicksman et al. (1994). More advanced fluidized bed models, based on momentum and mass conservation equations, are also reviewed by Glicksman et al. (1994). These investigations employ relevant empirical and semi-empirical correlations, which are inter alia used as supplemental constitutive equations for these hydrodynamic models of fluidization. These models are also used for a more subtle analysis of fluidization, including instabilities and transient regimes.

One of the important subjects of these studies is the instability of a statistically uniform fluidized bed, which causes large fluctuations in particle concentration. A natural and common speculation is that these instabilities lead to the formation of bubbles originating in the fluidized bed. Jackson (1963) showed that steady motion of a homogeneous gas-particle suspension including the gas and solid inertia and drag forces is always unstable. Wallis (1969) introduced the granular pressure that resists particle motion. He used simple model equations to conclude that the criterion for instability is that the kinematic wave speed exceeds the dynamic wave speed. Using physical arguments, Batchelor (1988) wrote down the momentum equation of solid-particle motion in a fluidized bed. This equation assumes a phenomenological barotropic dependence of the granular pressure on solid volume fraction with a coefficient representing, actually, the bulk modulus of elasticity. As a result, he generalized Wallis' criterion for instability. A comprehensive review of recent works on the subject can be found in the paper of Batchelor and Nitsche (1994). Nonlinear stability analyses of a uniformly fluidized bed are given in several studies (see Refs. Ganser and Drew, 1990; Harris and Crighton, 1994; Lammers and Biesheuvel, 1996 and papers cited therein).

Quantitative use of the momentum equation requires some insight into the physical origin of the effective elasticity of particle arrangement and calculation of the bulk modulus, governing the granular pressure.

In the kinetic theory of gases the pressure is induced from the randomly fluctuating motion of the molecules. It is, therefore, reasonable to expect that the granular pressure may arise from random motion of particles in situations in which their inertia is significant. In recent years, considerable attention has been focused on developing a kinetic theory for the rapid motion of granular materials. (For recent discussions, see Ref. Goldshtein and Shapiro, 1995). This theory deals with the motion of a suspension of particles undergoing solid-body collisions. The effect of the fluid on particle motion is neglected. Therefore, analysis of hydrodynamic interactions within a group of many particles is needed. Recently, such an analysis was performed by Koch (1990), who considered dilute gas–solid suspensions of small particles with low Reynolds number. The velocity distribution of the particles then appears to be nearly Maxwellian, if the particle Stokes number happens to be sufficiently high. This seems to be an immediate consequence of the significance of the hydrodynamic and solids interactions in interparticle exchange.

Elucidation of the very nature of fluctuations of the particle velocity lies within the focus of

several theoretical models. Buyevich (1994, 1997) and Buyevich and Kapbasov (1994) proposed a model according to which the random fluctuations are due to fluctuations of forces exerted on individual particles by the fluid. They considered fluctuations of particle concentration as a physical reason for fluctuations of hydrodynamic forces, which in turn affect the particle concentration distribution. Nonlinear dependence of those forces on the particle volume fraction leads to the occurrence of an additional source term in the average momentum equation, causing either particle acceleration or deceleration with respect to the mean flow.

Gidaspow and Huilin (1996) measured the granular temperatures in a circulating fluidized bed. Zenit et al. (1997) measured the collisional solid particle pressure in a uniform fluidized bed. It is shown, in particular, that the phenomenological dependence of the particulate pressure on the particle volume fraction suggested by Batchelor (1988) is in quantitative agreement with the experimental data, while the granular pressures reported by Buyevich and Kapbasov (1994) are significantly smaller than corresponding experimental values.

It should be noted that the Batchelor's barotropic dependence is applicable only to uniformly fluidized bed. Generally, such dependencies can be derived proceeding from kinetic models of particle fluctuation motions, and are to be different for different fluidization processes.

An alternative concept of particle velocity fluctuations was proposed by Goldshtik and Kozlov (1973), where concentration fluctuations were neglected. The fluctuating motion of the particles was attributed to the action of a Magnus lateral force exerted on particles that randomly rotate in the shear flow of the ambient gas. We shall show that this model enables us to obtain different barotropic dependencies of the particulate pressure on the particle volume fraction depending on the type of fluidization processes.

A specific goal of the present work is the analysis of different stationary regimes of the disperse fluidization in confined volumes. For this purpose the model of Goldshtik and Kozlov (1973) describing the fluctuations arising due to the Magnus force is further extended. We obtain a set of equations governing the granular temperature and the bulk modulus of a homogenous fluidized bed. These properties are expressed in terms of the particle volume fraction, mixture supply rate and properties of the gas and particles.

The paper is organized as follows. Equations describing the mean flow of a gas–solid suspension are derived in Section 2. An analysis of stationary regimes of fluidization in an infinite medium is given in Section 3. Theoretical and experimental studies of a fluidized bed in confined volumes is presented in Section 4. The stability problem of the stationary solutions in confined volumes is addressed in Section 5. Combined vibro- and gas-fluidization processes are investigated in Section 6.

2. One-dimensional model of a gas-fluidized bed

Some of the elements of the model proposed here may be found in the works of Batchelor (1988), Nigmatulin (1978), and Goldshtik and Kozlov (1973). In this section, we describe the general form of the equations that govern the mean particle and gas motion in the vertical direction. In parallel, we delineate the basic differences between the present model and the models developed in the previous studies.

The fluidizing medium under consideration is a gas, with density ρ_g^0. The particles are assumed to be identical, and of uniform density ρ_s^0. Both fluidizing gas and particles are incompressible, moreover $\rho_g^0/\rho_s^0 \ll 1$.

The fluidized bed is assumed to be statistically homogeneous in each horizontal plane. The mean particle velocity is vertical, and is not necessarily steady. The mean value of any property φ, which is denoted by $\langle\varphi\rangle$, is a spatially averaged value over a horizontal plane $y = \text{const}$ (see Fig. 1). Hence,

$$\varphi = \frac{1}{\mathrm{d}N}\sum_{\xi=1}^{\mathrm{d}N}\varphi(\xi) = \langle\varphi(\xi)\rangle \tag{1}$$

where $\varphi(\xi)$ corresponds to the center of xth particle, and $\mathrm{d}N$ is the total number of particles. In view of the horizontal homogeneity, this spatial average is equivalent to an ensemble mean (Batchelor, 1988).

Consider a control volume bounded by two horizontal planes (see Fig. 1) so that the distance between the planes is small compared with the distance over which the change in the mean number density $n(y',t')$ is appreciable. We assume that the particle average rotational velocity is zero. The translational velocity of the center of xth particle may be represented as

$$v_s'(\xi) = v_s' + w_s'(\xi), \tag{2}$$

where w_s' is the translational velocity fluctuation and $v_s'(y',t')$ is the mean particle velocity which is positive when directed upwards, along the y'-axis (see Fig. 1). Each particle rotates about its center with the velocity ω_s'. Using $\langle w_s'\rangle = \langle\omega_s'\rangle = 0$, we denote the following statistical properties

$$w_{s^*}'^2 = \langle w_s'^2(\xi)\rangle, \quad \omega_{s^*}'^2 = \langle\omega_s'^2(\xi)\rangle \tag{3}$$

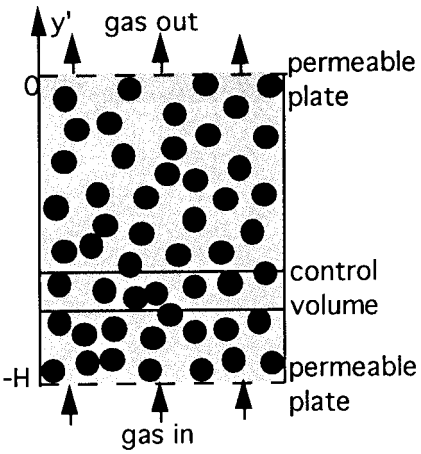

Fig. 1. Schematic of a fluidized bed with a coordinate system.

The averaging procedure, set down above, is similar to that used by Batchelor (1988) who considered fluidization processes, however, without particle rotation.

By virtue of the smallness of the fluid density $\rho_g^0/\rho_s^0 \ll 1$, the translational particle velocity fluctuations w'_{s^*} are much smaller than the average velocities of the relative particle to gas flow, that is

$$w'_{s^*} << v_{gs} = |v'_g - v'_s| \tag{4}$$

where v'_g is the mean gas velocity. The inertial properties of each particle are characterized by its mass m and moment of rotational inertia I. In particular, for uniform spheres of radius a, one has $m = 4\pi a^3 \rho_s^0/3$, $I = 2ma^2/5$. Hence, the kinetic energy of random motion, k'_s is

$$\rho_s^0 \alpha_s k'_s = \frac{1}{2} nm w'^2_{s^*} + \frac{1}{2} nI \omega'^2_{s^*}, \tag{5}$$

where α_s is the particle volume fraction, related to the voidage α_g by $(\alpha_s + \alpha_g) = 1$. The particle volume fraction may be expressed in terms of mean number density by the equation $\alpha_s = 4n\pi a^3/3$.

We assume equal rotational and translational rotational distribution between degrees of freedom. Thus, using Eq. (5) one obtains

$$\frac{1}{2} w'^2_{s^*} = \frac{1}{5} a^2 \omega'^2_{s^*} \tag{6}$$

This yields a relationship between the spatially averaged rotational and translational velocities

$$\omega'_{s^*} = \frac{w'_{s^*}}{a} \sqrt{\frac{5}{2}}, \tag{7}$$

and the following expression for the total average kinetic energy of particle random motion

$$k'_s = w'^2_{s^*}. \tag{8}$$

This equation is later on used for evaluation of the Magnus force (see Eqs. (14) and (15)) and the kinetic energy production (see Eqs. (16) and (27)).

The assumption of equipartition of the kinetic energy between the translational and rotational modes used above, corresponds to particle collisions as perfectly rough spheres. More realistic collisional models of granular materials, accounting for different particle roughness coefficients, range from perfectly rough to perfectly smooth spheres (see Refs. Goldshtein and Shapiro (1995), Lun and Savage (1987) and the papers cited therein). All these works, however, neglect the effect of the gas on particle motion.

We now consider the equation of state of the granular gas for a sufficiently concentrated disperse mixture, i.e. $\alpha_s > 0.1$. In this case, Enskog's approximate kinetic model of dense gases of identical spheres may be applied to calculate the equation of state of the granular gas (Hirschfelder et al., 1954)

$$p'_{s*} = \frac{1+e}{2}\frac{\rho_s^0 w_{s*}'^2}{2}\frac{\alpha_s}{1-\left(\frac{\alpha_s}{\bar{\alpha}_s}\right)^{1/3}}, \qquad \bar{\alpha}_s = 0.63 \tag{9}$$

where $\bar{\alpha}_s$ is a volume particle fraction of the most densely packed bed, e is the particle coefficient of restitution, p'_{s*} is the granular gas pressure. The effect of inelasticity on particle collisions is to decrease the granular pressure compared to the case of elastic collisions by the factor $(1+e)/2$. Note that granular shear stresses in fluidized beds are negligible.

The granular pressure, generally, consists of a purely kinetic part and a collisional transfer pressure part (Gidaspow, 1994; Goldshtein and Shapiro, 1995). The pure kinetic pressure is negligible for concentrated granular gases, and is not included in Eq. (9).

For formulation of the hydrodynamic equations for the average particulate and gas properties, we need to calculate the forces acting on the particles. Forces exerted by the gas on the particles, generally, include the drag force, the added mass force, the Basset force and the Magnus force. In our case, the added mass and the Basset forces are negligible because $\rho_g^0/\rho_s^0 \ll 1$.

For the spatially averaged drag force acting on the particle we use the following relationship (Goldshtik, 1972; Buyevich and Kapbasov, 1994)

$$f_\mu \equiv \langle f_\mu(\xi)\rangle = C_\mu \frac{\alpha_g^2}{\alpha_{g*}^2}\pi a^2 \frac{\rho_g^0 \upsilon_{gs}'^2}{2}. \tag{10}$$

Here, C_μ is a resistance coefficient of a single sphere and α_{g*} is the minimal gas passage area fraction, which can be approximated as (Goldshtik, 1972)

$$\alpha_{g*} = 1 - 1.17\alpha_s^{2/3}. \tag{11}$$

We restrict our attention to rapid gas flow through the fluidized bed so that the Reynolds number based on particle diameter is large, i.e.,

$$Re_{gs} = \frac{2\upsilon'_{gs}a}{\nu_g} >> 1 \tag{12}$$

where ν_g is the gas kinematic viscosity. In this case, C_μ is close to 1/2, and Eq. (10) takes on the form

$$f_\mu = \frac{1}{2}\frac{\alpha_g^2}{\alpha_{g*}^2}\pi a^2 \frac{\rho_g^0 \upsilon_{gs}'^2}{2}. \tag{13}$$

The Magnus force arises due to particle rotation. The expression for this force was first obtained for very small Reynolds numbers by Rubinow and Keller (1961). A review of empirical correlations, which are valid for small and moderate Reynolds numbers, is given in the recent work of Lun and Lin (1997). We will, however, use the expression of Goldshtik and Sorokin (1968)

$$\mathbf{f}_{\mathrm{M}}(\xi)=\frac{8}{3}\pi a^3\rho_{\mathrm{g}}^0\Big[\mathbf{v}'_{\mathrm{gs}}(\xi)\times\omega(\xi)\Big], \tag{14}$$

valid for very large Reynolds numbers.

One can show that the spatially averaged Magnus force $\langle\mathbf{f}_{\mathrm{M}}\rangle$ is of the order $O(w'_{\mathrm{s}*}\omega'_{\mathrm{s}*})$. Then it follows from Eqs. (13) and (14) that the ratio of this force to the drag force is

$$\frac{f_{\mathrm{M}}}{f_\mu}=O\left(\frac{w'_{\mathrm{s}*}\omega'_{\mathrm{s}*}}{\upsilon'^2_{\mathrm{gs}}}\right), \tag{15}$$

and it, therefore, can be neglected in the hydrodynamic momentum equations by virtue of Eqs. (4) and (7). It should be noted, however, that the Magnus force plays an important role in the generation of the kinetic energy of random particle motion. Evolution of this property is governed by the kinetic energy conservation equation which involves terms associated with production and dissipation of the fluctuation energy due to the interaction with the ambient gas and interparticle collisions.

Energy production due to Magnus forces f_{M} determined by Eq. (14) may be estimated by assuming the angles between vectors $\mathbf{v}'_{\mathrm{gs}}(\xi)$ and $\omega'_{\mathrm{s}}(\xi)$, and also between vectors $[\mathbf{v}'_{\mathrm{gs}}(\xi)\times\omega'_{\mathrm{s}}(\xi)]$ and $\mathbf{w}'_{\mathrm{s}}(\xi)$ to be equal to $\pi/4$ (Goldshtik and Kozlov, 1973). Then, using Eq. (7) one obtains for the generated power Q_+ in unit volume

$$Q_+=\langle\mathbf{f}_{\mathrm{M}}(\xi)\mathbf{w}'_{\mathrm{s}}(\xi)\rangle=\frac{4}{3}\sqrt{\frac{5}{2}}\rho_{\mathrm{g}}^0\pi a^2\upsilon'_{\mathrm{gs}}w'^2_{\mathrm{s}*}. \tag{16}$$

Assuming an isotropic distribution of the translational fluctuation velocity, $w'_{\mathrm{s}}(\xi)$ one obtains for the viscous dissipation (Nigmatulin, 1978)

$$\langle\mathbf{f}_\mu(\xi)\mathbf{w}'_{\mathrm{s}}(\xi)\rangle=-\frac{3}{8}\rho_{\mathrm{g}}^0\pi a^2\frac{\alpha_{\mathrm{g}}^2}{\alpha_{\mathrm{g}^*}^2}\upsilon'_{\mathrm{gs}}w'^2_{\mathrm{s}*}. \tag{17}$$

The ratio of the dissipated energy to the produced energy is

$$\frac{\langle f_\mu(\xi)\omega'_{\mathrm{s}}(\xi)\rangle}{\langle f_{\mathrm{M}}(\xi)\omega'_{\mathrm{s}}(\xi)\rangle}=0.18\frac{\alpha_{\mathrm{g}}^2}{\alpha_{\mathrm{g}^*}^2} \tag{18}$$

One can, therefore, see that for the granular gas, except in the vicinity of the close-packed state, the viscous kinetic energy dissipation is significantly smaller than the kinetic energy production due to the Magnus force.

Eq. (16) implies that the energy production term is proportional to the translational kinetic temperature. A kinetic model for a dilute gas–solid suspension, suggested by Koch (1990), yields that for very small Reynolds numbers the source term in the granular kinetic energy equation, arising from particle hydrodynamic interactions, is inversely proportional to the square root of the temperature. Buyevich (1994, 1997) attributed the generation of the fluctuation energy to particle concentration fluctuations. His model disregards particle rotation, as does the model of Koch (1990). Buyevich obtained the source term in the energy equation as proportional to the square root of the temperature. We point out that in contrast with the

present model the theories of Buyevich (1997), and Koch (1990) are applicable for very small Reynolds numbers.

Consider kinetic energy losses due to particle collisions. There are three possible reasons, why particle collisions cause kinetic energy dissipation. The first reason is the work of the viscous hydrodynamic forces stemming from the jump-like changes in the gas and particle velocity that accompany any collision. These losses are negligible when $\rho_g^0/\rho_s^0 \ll 1$. The second reason is the action of surface friction that, generally, impedes sliding of impacting spheres during oblique collisions. In our model, the particles are assumed perfectly rough spheres. In this case, no kinetic energy is dissipated due to surface friction. Part of the translational kinetic energy is converted into particle rotational kinetic energy during oblique collisions. Note that the viscous dissipation of the rotational kinetic energy is negligible at the high Reynolds numbers Re_{gs} considered in this study.

The third reason of the kinetic energy dissipation is due to the inelasticity of collisions when the coefficient of restitution, e, is smaller than unity. Considerable attention has previously been focused on developing models of this mechanism of the collisional dissipation (see Ref. Goldshtein and Shapiro, 1995; Lun and Savage, 1987). We consider concentrated dispersions of inelastic perfectly rough spheres and use for the dissipated power per unit volume Q_- the relevant equation

$$Q_- = \frac{1-e^2}{8}\frac{\rho_s^0}{a}\frac{\alpha_s^{4/3}}{\bar{\alpha}_s^{1/3}\left(1-\left(\frac{\alpha_s}{\bar{\alpha}_s}\right)^{1/3}\right)} w_{s^*}'^3 \tag{19}$$

The assumptions set down at the beginning of this section together with the expressions for the forces and kinetic energy production and dissipation are further used in the hydrodynamic equations. These equations may be obtained by the method of spatial averaging (Nigmatulin, 1978). As a result one arrives at the following one-dimensional equations:

gas mass continuity equation
$$\frac{\partial \alpha_g}{\partial t'} + \frac{\partial \alpha_g v_g'}{\partial y'} = 0 \tag{20}$$

particle conservation equation
$$\frac{\partial \alpha_s}{\partial t'} + \frac{\partial \alpha_s v_s'}{\partial y'} = 0 \tag{21}$$

gas momentum balance equation
$$\frac{\partial p_g'}{\partial y'} - n f_\mu - \rho_g^0 \alpha_g g = 0 \tag{22}$$

particle momentum equation
$$\rho_s^0 \alpha_s \left(\frac{\partial v_s'}{\partial t'} + v_s' \frac{\partial v_s'}{\partial y'}\right) = -\frac{\partial p_{s^*}'}{\partial y'} + n f_\mu - \rho_s^0 \alpha_s g \tag{23}$$

particle kinetic energy equation
$$\rho_s^0 \alpha_s \left(\frac{\partial k_s'}{\partial t'} + v_s' \frac{\partial k_s'}{\partial y'}\right) = -p_{s^*}' \frac{\partial v_s'}{\partial y'} + Q_+' - Q_-' \tag{24}$$

This system is supplemented by the following constitutive equations

$$f'_{\mu} = \frac{1}{2}\frac{\alpha_g^2}{\alpha_{g^*}^2}\pi a^2 \frac{\rho_g^0 v_{gs}'^2}{2}, \tag{25}$$

$$p'_{s^*} = \frac{1+e}{2}\frac{\rho_s^0 k'_s}{2}\frac{\alpha_s}{1-\left(\frac{\alpha_s}{\bar{\alpha}_s}\right)^{1/3}}, \tag{26}$$

$$Q'_{+} = \frac{4}{3}\sqrt{\frac{5}{2}}\rho_g^0 n\pi a^2 v'_{gs} k'_s \tag{27}$$

$$Q'_{-} = \frac{1-e^2}{8}\frac{\rho_s^0}{a}\frac{\alpha_s^{4/3}}{\bar{\alpha}_s^{1/3}\left(1-\left(\frac{\alpha_s}{\bar{\alpha}_s}\right)^{1/3}\right)} k_s'^{3/2} \tag{28}$$

Note that the inertial terms in the gas momentum Eq. (22) are neglected, as well as the viscous dissipation term in the Eq. (24) for the fluctuation energy. Eqs. (27) and (28) are obtainable from Eqs. (16) and (19) upon using relations (7) and (8). We use these equations for the analysis of steady state fluidized beds and unsteady fluidization regimes.

3. Steady-state fluidized bed in an unconfined volume

Solid particles at rest in a vertical cylinder which are supported by a permeable gas distribution plate form a packed bed. If the gas is forced through the plate from below, the bed remains packed until the flow rate reaches a certain critical value. At this value the bed expands a little and becomes fluidized. The voidage, α_g increases and the interstitial gas velocity decreases and becomes lower value needed for the particles to be carried out of the bed. As a result a new equilibrium regime is reached, when particles are quiescent on the average, $v'_s = 0$, however, they are engaged in random motion ($w'_{s^*} \neq 0$, $\omega'_{s^*} \neq 0$). Such a bed is called a bed at minimum fluidization.

Increase of the gas flow rate causes the bed to expand further. Under certain conditions this expansion is uniform, and the bed remains statistically homogeneous, with the number density of the particles taking just the value required for the weight of a particle to be balanced by the mean drag force exerted by the gas. The particles can be carried out by the gas and recycled to the bed entrance forming a recirculating fluidized bed. Actually, the particles, dispersed throughout the fluid, likewise fall vertically relative to the fluid under the action of gravity. Such a homogenous stationary fluidized bed ($\alpha_g = \text{const}$) is similar to a homogeneous cloud of particles sedimenting in a quiescent gas (Batchelor, 1988). We first apply the governing equations set out in the previous section to this classical situation.

3.1. Homogenous steady state fluidized bed

We look for a solution of Eqs. (20)–(28), where all functions are t and y independent, i.e., constant quantities. Equations of mass conservation (20) and (21) are integrated for homogeneous stationary fluidization, leading to

$$\alpha_g v'_g + \alpha_s v'_s = v_0, \tag{29}$$

In the above equation all the parameters are constant. Here v_0 is the velocity of the gas–solid mixture at the inlet to the bed. If one considers particle sedimentation in a quiescent gas, v_0 should be put equal to zero. In a homogeneous fluidized bed, the velocity v_0 determines the mean volumetric flux of the mixture across any specified horizontal surface. When particle entrainment (carry over) takes place, the solids must be recycled or replaced by fresh material to maintain steady-state operation. In this context, the quantity v_0 represents the recirculation flux. Eq. (29) enables one to express the gas velocity in terms of particle velocity and volume fraction.

Eqs. (23) and (24) of the granular phase momentum and energy yield in the present case

$$nf_\mu - \rho_s^0 \alpha_s g = 0 \tag{30}$$

$$Q'_+ - Q'_- = 0 \tag{31}$$

Furthermore, the mean particle velocity is a function of α_s, i.e., $v'_s(\alpha_s)$ This is obtained using Eqs. (25), (29) and (30):

$$v'_s = v_0 + \left(1 - 1.17\alpha_s^{2/3}\right) u_t \tag{32}$$

where

$$u_t = \left(\frac{16}{3}\frac{\rho_s^0}{\rho_g^0} ag\right)^{1/2}. \tag{33}$$

Here, u_t is the terminal velocity of a single particle in a quiescent gas. Using Eqs. (27) and (28), one obtains from Eq. (31) the expression for the fluctuation kinetic energy

$$k_s'^{1/2} = 8\sqrt{\frac{5}{2}}\frac{\rho_g^0}{\rho_s^0}\frac{0.86 u_t}{1-e^2}\frac{\left(1 - 1.17\alpha_s^{1/3}\right)\left(1 - 1.17\alpha_s^{2/3}\right)}{\alpha_s^{1/3}(1-\alpha_s)} \tag{34}$$

Note that although this expression is explicitly independent of v_0, it is valid for $v_0 \geq u_t$. This inequality is in fact the condition of validity of the homogeneous stationary solution discussed here. We can now substitute Eq. (34) into Eq. (26) to obtain the barotropic dependence specific for a uniform fluidized bed.

4. Fluidized bed in a confined volume-theory and experiment

Here, we consider the motion of particles and gas in a cylindrical space between two

permeable plates separated by a distance H. If the plates are made of an elastic material and the particles are elastic enough, they bounce off the upper plate when $v_0 > u_t$. The reflected particles collide with those moving upward and force them to move downward. We will analyze whether an equilibrium particle distribution can take place in the confined volume under such conditions, in which the particles while moving randomly, have zero net velocity on the average, i.e., $v_s' = 0$. We show that such a regime can indeed be realized and call it a disperse fluidized bed in a confined volume. Generally, this disperse bed is nonhomogenous, i.e., $\alpha_s = \alpha_s(y')$

4.1. Theoretical study

We assume that the condition $v_s' = 0$ is valid throughout the whole bed up to the boundaries $y' = 0, -H$. This assumption complies with the obvious boundary conditions of impenetrability of the distributor plates. Physically this means that the plates are sufficiently rigid and their collision with particles are sufficiently elastic so that $v_s' = 0$ also at the boundaries. These requirements do not preclude the occurrence of a situation where the particles are attached (i.e., with $k_s' = 0$) to the upper (or lower) plate. This situation can take place when the particle kinetic energy dissipation dominates over the kinetic energy production and all the particles form an inverted packed bed (plug) at the upper plate. We show below that such a regime is indeed predicted by our model.

Since $v_s' = 0$, the integral of Eqs. (20) and (21) takes now the form

$$\alpha_g v_g' = v_0 \tag{35}$$

here v_0 is the velocity of the gas at the inlet to the bed, at $y' = -H$ where $\alpha_g = 1$ (Fig. 1). Furthermore, Eqs. (23) and (24) combined with Eqs. (25), (27) and (28) and $v_s' = 0$ yield

$$\frac{dp_{s*}'}{dy'} = \rho_s^0 g \alpha_s \left(\frac{U_0^2}{\left(1 - 1.17\alpha_s^{2/3}\right)^2} - 1 \right) \tag{36}$$

$$k_s'^{1/2} = k_{s*}^{1/2} \frac{1 - 1.17\alpha_s^{1/3}}{(1 - \alpha_s)\alpha_s^{1/3}} \tag{37}$$

where

$$U_0 = v_0 / u_t \tag{38}$$

is a dimensionless parameter of the disperse bed and

$$k_{s^*}^{1/2} = 8\sqrt{\frac{5}{2}} \frac{\rho_g^0}{\rho_s^0} \frac{0.86 v_0}{1 - e^2} \tag{39}$$

here, k_{s^*} is the characteristic value of the fluctuation energy.

Substituting Eq. (37) into Eq. (26) yields the equation for the granular pressure in terms of the particle fraction α_s

$$p'_{s^*}(\alpha_s) = \frac{1+e}{2}\frac{\rho_s^0 k_{s^*}}{2}\psi(\alpha_s), \tag{40}$$

where

$$\psi(\alpha_s) = \frac{\alpha_s^{1/3}\left(1 - 1.17\alpha_s^{1/3}\right)}{(1-\alpha_s)^2} \tag{41}$$

It follows, thus, that there exists a barotropic relationship between the granular pressure and the particle fraction, which is a direct consequence of the equilibrium between the production and dissipation of the granular kinetic energy. As such, the pressure $p'_{s^*}(\alpha_s)$ is equal to zero at $\alpha_s = 0$ and $\alpha_s = \bar{\alpha}_s = 0.63$ and it has a maximum at $\alpha = \alpha_{s\psi} = 0.32$. Eq. (26), and consequently, Eq. (40) are both valid for $\alpha_s > 0.1$.

Note that this barotropic relationship is different from that for a homogeneous fluidized bed, which was discussed in Section 3.

We now define the dimensionless variables

$$y = \frac{y'}{H}, \quad k_s = \frac{k'_s}{k_{s^*}}, \quad p_s = \frac{p'_{s^*}}{\rho_s^0 k_{s^*}} \tag{42}$$

Using Eq. (42) and substituting Eq. (40) into Eq. (36) yields

$$\frac{d\alpha_s}{dy} = \Pi_g \frac{\alpha_s\left(\dfrac{U_0^2}{\left(1 - 1.7\alpha_s^{2/3}\right)^2} - 1\right)}{\dfrac{d\psi}{d\alpha_s}}, \tag{43}$$

where Π_g is a dimensionless group

$$\Pi_g = \frac{4gH}{k_{s^*}(e+1)} \tag{44}$$

Using Eqs. (40) and (41), one can rewrite Eq. (43) in the form

$$\frac{d\zeta}{dy} = -1.17\Pi_g \frac{K(\zeta)}{\zeta - \zeta_\psi}\zeta^3, \tag{45}$$

where

$$\zeta = \alpha_s^{1/3}, \quad K(\zeta) = \frac{\left(\alpha_{g^*} + U_0\right)\alpha_g^3\left(\zeta^2 + \dfrac{U_0 - 1}{1.17}\right)}{\alpha_{g^*}^2\left(4.64\zeta^3 - 1.89\zeta^2 - 1.27\zeta + 1.47\right)} > 0, \tag{46}$$

and α_{g^*} given by Eq. (11) is expressible via ζ in the form

$$\alpha_{g^*} = 1 - 1.17\zeta^2. \tag{47}$$

Note that $K(\zeta)$ is a positive function since $U_0 > 1$.

The boundary condition for ζ posed at the lower supporting plate $y = -1$ is

$$y = -1: \quad \zeta = \zeta_0 \tag{48}$$

where ζ_0 is some boundary value. An integral condition

$$\int_{-1}^{0} \alpha_s(y)\,\mathrm{d}y = \frac{H_p}{H}\bar{\alpha}_s = 0.63\frac{H_p}{H} \tag{49}$$

is imposed upon $\alpha_s(y)$ and the height H_p of the resting nonfluidized (packed) bed. In the course of integration of Eq. (43) a value ζ_0 is to be chosen to satisfy Eq. (49).

Eqs. (30) and (31) have a trivial stationary solution $k_s' = 0$, corresponding to the packed bed ($\alpha_s = \bar{\alpha}_s$). Regarding the packed bed adjacent to the lower distribution plate, this solution may be unstable if gas velocities are sufficiently large to cause fluidization. This solution describes also a plug adjacent to the upper plate. It is clear that in the limiting case when packed solids completely fill the confined cylinder space, this solution is unique.

Consider now the case where the height of the packed bed is only slightly less than H ($H - H_p \ll 1$) (deep bed). Note first that an integral curve of the differential Eq. (45) cannot intersect the line $\zeta = \zeta_\psi$, since at this line the derivative $\mathrm{d}\zeta/\mathrm{d}y$ tends to infinity. In this case the boundary value $\zeta = \zeta_0$ lies in the region $\bar{\zeta} > \zeta > \zeta_\psi$. Hence, $\mathrm{d}\zeta/\mathrm{d}y<0$, i.e., the particle fraction decreases in the direction of gas flow. Peculiarities of the behavior of the integral curves depend on the dimensionless group Π_g given by (44). This group is very small for small volume sizes, H, or high fluctuation energies; i.e., for very elastic spheres, $e \leq 1$. Note, that in this case the parameter U_0 should not to be very large. This condition is fulfilled for sufficiently large particles but not large gas supply velocity, v_0. On the contrary, Π_g is very large for large volume sizes or for inelastic spheres. Note, that the condition $U_0 > 1$ ($v_0 > u_t$) applies then for sufficiently small particles. Curves 1, 2 in Fig. 2(a) correspond to $\Pi_g \ll 1$ and $\Pi_g \gg 1$, respectively. We have seen that at $\Pi_g \ll 1$ there exists a stationary solution. The solution corresponds to the deep fluidized bed with the solid fraction decreasing along the bed height.

On the other hand, when $\Pi_g \gg 1$ the value ζ decreases rapidly with y reaching $\zeta = \zeta_\psi$ within the bed (see also Eq. (45)) at $y = y_{max}$. For $y > y_{max}$ one has $\zeta = 0$, i.e., no particles are present in the upper part of the bed $y_{max}<y<0$ (see Fig. 2(a), curve 2). This is impossible for two reasons: firstly, since $U_0 > 1$ the particles are carried upwards thereby inevitably reaching the upper plate, the feature which is not reproduced by this solution. Secondly, the distribution represented by curve 2 in Fig. 2(a) is impossible since it does not satisfy the integral condition (49) at least at sufficiently large Π_g (low gas velocities and small inelastic particles).

Let us now consider a flow where the total solid mass is small, $H_p/H<1$ (shallow bed) so that the boundary value $\zeta = \zeta_0$ lies in the region $\zeta<\zeta_\psi$. Hence, $\mathrm{d}\zeta/\mathrm{d}y > 0$, i.e., the particle fraction increases in the direction of gas flow. Curves 3 and 4 in Fig. 2(b) correspond to $\Pi_g \ll 1$ and $\Pi_g \gg 1$, respectively. We see that at $\Pi_g \ll 1$ there exists a stationary solution corresponding to the disperse fluidized bed with particle fraction increasing along the height.

Similarly to the conclusion drawn above for the deep bed, no physically plausible solution exists when $\Pi_g \gg 1$, also for the shallow bed (see curve 4 in Fig. 2(b)).

Thus, one can summarize that the stationary Eqs. (45) and (46) predict four typical regimes of fluidization in confined volumes. Out of these regimes, the two, corresponding to $\Pi_g \gg 1$

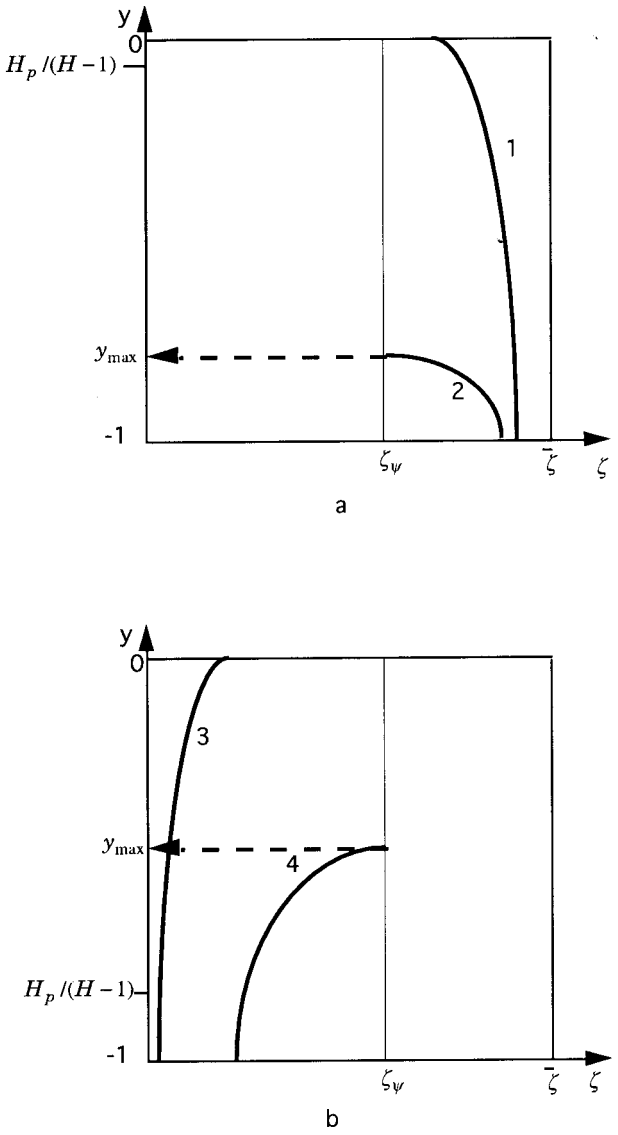

Fig. 2. Integral curves of differential equation (43) for different mass contents and values of the dimensionless group Π_g: (a) deep disperse fluidized bed; (b) shallow disperse fluidized bed. Position $y = H_p/(H-1)$ shows the particle mass content of the packed beds. Curves 1, 3 correspond to $\Pi_g \ll 1$, large and small particle mass contents, respectively. Curves 2, 4 correspond to $\Pi_g \gg 1$, large and small particle mass contents, respectively.

are not physical. However, in cases where $\Pi_g \gg 1$ our equations predict the existence of the plug regime, where all the particles form an inverted packed bed (plug) adjacent to the upper plate. The two regimes corresponding to $\Pi_g \ll 1$ will be analyzed for stability. As we will see, the deep fluidized bed (with particle volume fraction decreasing along the bed height) is unstable at least when $\Pi_g \to 0$. Note, that the realization of the disperse regime represented by curve 3 in Fig. 2(b) for a gas–solid system, requires very shallow beds (small H) and/or very

elastic large particles. Alternatively, one can envision these regimes in liquid-fluidized beds where ρ_g and ρ_s may be of the same order of magnitude, thereby yielding small Π_g.

Finally, note that in the limiting situation $\Pi_g \to 0$ the non-uniformity of the disperse fluidized beds diminishes. In this case one obtains from Eq. (45) the simple solution

$$\alpha_s = \alpha_{sa} = \bar{\alpha}_s \frac{H_p}{H} \tag{50}$$

corresponding to the fully disperse fluidized bed.

Regions of existence of plug and disperse regimes in terms of parameters Π_g, U_0 for several values of H_p/H are shown in Fig. 3. The disperse regime corresponds to the regions under the curves. The numerical procedure of integration of differential Eq. (45) subject to integral condition (49) is described in the Appendix A.

4.2. Experimental study

An experiment has been designed in order to show the existence of the disperse regime of fluidization in a confined volume. The experimental set-up is shown in Fig. 4. The test section of the apparatus consists of a vertical tube, 27 cm long and 10 cm in internal diameter. It is confined from above and from below by gas permeable distribution plates. Air is supplied by a high pressure blower. The air velocity, which was measured by hot wire anemometer, ranges from 4 to 17 m/s. 500 glass spheres of 0.34 cm in diameter with a restitution coefficient 0.89 was placed on the lower plate, which corresponded to the ratio $H_p/H = 0.0125$. Minimum fluidization had been observed at an air velocity of about 4.6 m/s. The onset of fluidization had been observed at the velocity of 10–11 m/s, with the pressure drop across the bed 5 mm H_2O. This velocity lied well below the terminal velocity (in our case 13.8 m/s), when a well developed fluidization had been obtained, but the particles did not bounce back from the upper distributor plate. Further, increase of velocity up to 15–16 m/s yielded the regime of disperse fluidization in a confined volume with particle bouncing (see photograph in Fig. 5). A slight increase (of order 0.2 m/s) of the air velocity above 16 m/s led to an instantaneous

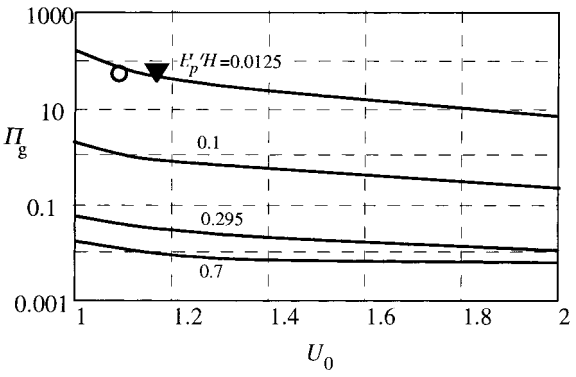

Fig. 3. Dimensionless height of the fluidized bed as a function of fluidization velocity.

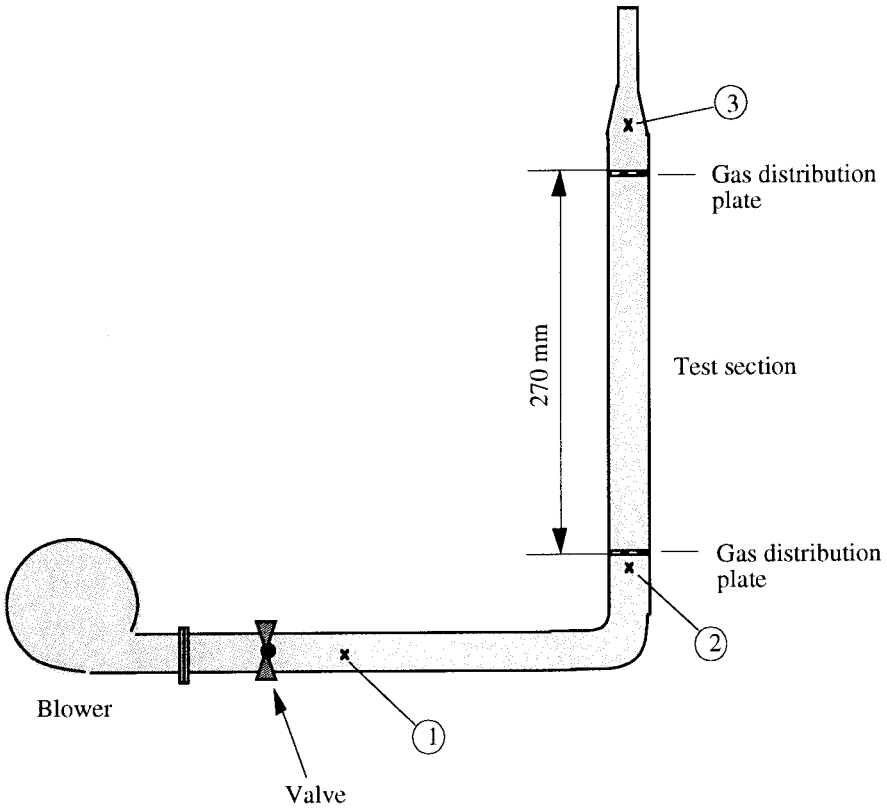

Fig. 4. Schematic of the experimental set-up. p_1, p_2, p_3 denote pressure measurement taps.

transition from dispersed to inverted packed regime (a plug adjacent to the upper plate). In this regime the pressure drop was about 200–230 mm H_2O.

Calculations by Eqs. (39) and (44) yield the value of the dimensionless parameter $\Pi_g = 37.3$. The above two regimes (namely, disperse and plug) corresponding to the respective velocities of 15 and 16 m/s are marked in Fig. 3. One can see that the onset of the plug regime (filled triangle) is well described by the theoretical curve of $H_p/H = 0.0125$. The disperse regime (hollow circle) is located below this curve, i.e., within the disperse regime domain. The experiments were performed for the systems with low particle concentrations of up to about 0.25 particles/cm^3. In such systems the particle concentration was found to be nonuniform. This nonuniformity amounted to about few percents.

The flow velocity range in the experiments was limited by the performance of the blower. The velocity could not be increased above 20 m/s. At these regime the air pressure supplied by the blower was not sufficiently high to achieve dispersed regimes in systems with higher solid fractions. The dense systems according to our theoretical analysis are unstable and, hence, should be investigated. These experiments as well as the analysis of higher solid fractions and their stability are the subjects of further investigation.

Fig. 5. Photograph of the disperse fluidized regime in a confined volume of the height $H = 27$ cm, containing one monolayer of glass beads (restitution coefficient $e = 0.89$) of diameter 3.4 mm; air velocity 15 m/s.

5. Stability of stationary fluidized beds in a confined volume

The stability of a fluidized bed was considered in the case of an infinite region. Here, we use the theory developed above to treat this problem in a confined volume. Generally, a stationary disperse fluidized bed in a confined volume has a nonuniform concentration distribution. However, we consider this problem in the limiting case $\Pi_g \to 0$ where the bed is homogeneous, i.e., solution (50) applies.

For the analysis of the stability of this solution, we define the following dimensionless variables

$$t = \frac{t'}{t_*}, \quad \upsilon_s = \frac{\upsilon_s' t_*}{H}, \tag{51}$$

where $t_* = H/k_{s*}^{1/2}$ is the characteristic propagation time of the disturbances of the particle fluctuation energy. Then, using Eqs. (42) and (51) one can rewrite Eqs. (21), (23), (24), (26)–(29) in the respective forms

$$\frac{\partial \alpha_s}{\partial t} + \frac{\partial \alpha_s \upsilon_s}{\partial y} = 0 \tag{52}$$

$$\alpha_s \frac{\partial v_s}{\partial t} + \alpha_s v_s \frac{\partial v_s}{\partial y} + \frac{\partial p_s}{\partial y} = 0 \tag{53}$$

$$\alpha_s \frac{\partial k_s}{\partial t} + \alpha_s v_s \frac{\partial k_s}{\partial y} + p_s \frac{\partial v_s}{\partial y} = Q_+ - Q_- \tag{54}$$

$$Q_+ = \sqrt{\frac{5}{2}} \frac{\rho_g^0}{\rho_s^0} \frac{v_o}{k_{s^*}^{1/2}} \frac{H}{a} \frac{\alpha_s}{1-\alpha_s} |1 - \frac{k_{s^*}^{1/2}}{v_0} v_s| k_s \tag{55}$$

$$Q_- = \frac{1-e^2}{8} 1.17 \alpha_s^{1/3} \frac{\alpha_s}{1 - 1.17\alpha_s^{1/3}} \frac{H}{a} k_s^{3/2} \tag{56}$$

$$p_s = \frac{1+e}{2} \frac{k_s}{2} \frac{\alpha_s}{1 - 1.17\alpha_s^{1/3}} \tag{57}$$

We investigate the stability of the stationary solution

$$\alpha_s = \alpha_{sa}, \quad v_s = 0,$$

$$k_{sa}^{1/2} = \frac{1 - 1.17\alpha_{sa}^{1/3}}{(1-\alpha_{sa})\alpha_{sa}^{1/3}} \tag{58}$$

We now assume the perturbation of the stationary solution (58) to be of the form

$$\alpha_s(t,y) = \alpha_{sa} + \alpha_{st}(t,y), \quad v_s(t,y) = v_{st}(t,y), \tag{59}$$

assuming that the kinetic energy obeys the equilibrium dependence Eq. (37). This assumption enables one to exclude the kinematic energy equation from the stability analysis. All terms of the governing Eqs. (52) and (53) vanish in the case of the homogeneous bed. Using Eqs. (36), (37) and (57), one obtains the linearized equations for the small perturbation quantities α_{st} and v_{st},

$$\frac{\partial \alpha_{st}}{\partial t} + \alpha_{sa} \frac{\partial v_{st}}{\partial y} = 0 \tag{60}$$

$$\alpha_{sa} \frac{\partial v_{st}}{\partial t} + P(\alpha_{sa}) \left(\alpha_{s\psi}^{1/3} - \alpha_{sa}^{1/3} \right) \frac{\partial \alpha_{st}}{\partial y} = 0$$

where $P(\alpha_{sa})$ is a positive function

$$P(\alpha_{sa}) = \frac{1+e}{4} \frac{4.64\alpha_{sa} - 1.89\alpha_{sa}^{2/3} - 1.27\alpha_{sa}^{1/3} + 1.47}{3\alpha_{sa}^{2/3}(1-\alpha_{sa})^3} \tag{61}$$

The equation system (60) may be easily transformed into a single equation which for the

velocity perturbation is

$$\frac{\partial^2 v_s}{\partial t^2} - P(\alpha_{sa})\left(\alpha_{s\psi}^{1/3} - \alpha_{sa}^{1/3}\right)\frac{\partial^2 v_s}{\partial y^2} = 0 \tag{62}$$

Note that Eq. (62) is hyperbolic in the region $\alpha_{sa}<\alpha_{s\psi}$ and elliptic in the region $\alpha_{sa} > \alpha_{s\psi}$.

Any small disturbance of a homogeneous disperse bed may be resolved into Fourier components which evolve independently. We, therefore, consider a disturbance that varies sinusoidally with y with the wave number K. In order to satisfy a boundary condition on the velocity $v_{st} = 0$ at $y = 0$ and $y = -1$, and the integral mass condition (49), we put

$$v_{st} = A\sin(m\pi y)e^{ict}, \quad \alpha_{st} = B\cos(m\pi y)e^{ict} \tag{63}$$

where A and B are constants and c is a complex number. Substitution in (60) gives the condition for the existence of a non-zero solution for A and B in the form

$$c^2 = (\pi m)^2 P(\alpha_{sa})\left(\alpha_{s\psi}^{1/3} - \alpha_{sa}^{1/3}\right) \tag{64}$$

One can see that a disturbance with an exponentially growing amplitude exists if

$$\alpha_s > \alpha_{s\psi} \tag{65}$$

This means that for the very concentrated mixtures ($H_p/H > \alpha_{s\psi}/\bar{\alpha}_s \sim 0.5$) the fully disperse bed in a confined volume is absolutely unstable. It is explained by the fact that in the region $\alpha_s > \alpha_{s\psi}$ the bulk modulus of elasticity of the granular phase is negative, $dp_s/d\alpha_s<0$. Any perturbation would continue to grow under the ensuing pressure drop. As a result, an initially homogeneous state of the disperse bed would eventually be transformed into an inhomogeneous unsteady pattern of different concentrations. One could anticipate that the inhomogeneous disperse bed with decreasing volume fraction, corresponding to $\alpha_s > \alpha_{s\psi}$ (see Section 4), will be unstable as well. This result accords with the instability of the homogeneous distribution of particles sedimenting in unconfined volumes (Batchelor, 1988).

A more general stability analysis of the nonbarotropic case, where the energy equation should be incorporated, yields similar results. We omit this treatment, but note that the effect of nonequilibrium energy distribution in a fluidized bed is to bring an additional decaying (stable) mode (see Ref. Koch, 1990).

6. Combined vibro- and gas-fluidized beds

It is well-known that vibrations of a plate supporting a packed layer of solid particles result under certain conditions in vibro-fluidization (Goldshtein et al., 1995). One may anticipate that vibrations of the upper porous plate, confining the vertical cylinder from above, can affect fluidization processes described in Section 4.

We first study the influence of small amplitude vibrations on a confined fluidized beds in disperse region. Let the upper plate perform the harmonic vibrations with an angular frequency ω and an amplitude h_a, where

$$h_a/H<<1. \tag{66}$$

Then, the boundary conditions on the mean particle velocity are to be given as follows:

$$\upsilon_s = 0 \quad \text{at} \quad y = -1$$

$$\upsilon_s = \varepsilon\cos\delta y \quad \text{at} \quad y = 0 \tag{67}$$

where ε and δ are the dimensionless groups

$$\varepsilon = \frac{\omega h_a}{k_{s^*}^{1/2}}, \quad \delta = \frac{\omega H}{k_{s^*}^{1/2}} \tag{68}$$

defined in accordance with the dimensionless variables determined by Eqs. (42) and (51). Note that the small term $h_a/H\sin\delta y$ was neglected in Eq. 67, which is justified by the smallness of the vibration amplitude.

It is clear that under such conditions particles are engaged in a mean motion ($\upsilon_s \neq 0$) in addition to the random fluctuations.

In addition to condition (66) we assume that the vibrational amplitude is sufficiently small, so that the dimensionless group ε is a small parameter of the problem, i.e., $\varepsilon \ll 1$. In such circumstances, the governing Eqs. (52)–(57) can be linearized about the stationary solution characterized by the zero mean particle velocity, $\upsilon_s = 0$. For the sake of simplicity we consider the effect of vibrations on the fully disperse, homogeneous fluidized bed ($\Pi_g \to 0$). Moreover, we study the pure hydrodynamic problem assuming, as in the stability problem analysis, that the kinetic energy obeys the equilibrium dependence (37). The governing equations are now reduced to Eq. (60). We seek a solution in the form

$$\upsilon_s(y,t) = \varepsilon\upsilon_{st}(y,t), \quad \alpha_s(y,t) = \alpha_{sa} + \varepsilon\alpha_{st}(y,t) \tag{69}$$

where

$$\upsilon'_{st} = V(y)\cos\delta t, \quad \alpha_{st} = \Phi(y)\sin\delta t \tag{70}$$

here $V(y)$ and $F(y)$ are functions to be determined. Boundary conditions (67) yield

$$V(-1) = 0, \quad V(0) = 1 \tag{71}$$

Substitution of Eq. (70) in Eq. (60) gives

$$V'' + \lambda V = 0$$

$$\Phi = -\frac{\alpha_{sa}}{\delta}V' \tag{72}$$

where prime denotes a derivative with respect to y, and λ is the following dimensionless group

$$\lambda = \frac{\delta^2}{P(\alpha_{sa})\left(\alpha_{s\psi}^{1/3} - \alpha_{sa}^{1/3}\right)} \tag{73}$$

In the region $\alpha_{sa}<\alpha_{s\psi}$ one has $\lambda > 0$. Then, the solution of the problem (72) and (71) is

$$V(y) = \frac{\cos\sqrt{\lambda}}{\sin\sqrt{\lambda}}\sin\sqrt{\lambda}y + \cos\sqrt{\lambda}y$$

$$\Phi(y) = -\frac{\alpha_{sa}\sqrt{\lambda}}{\delta}\left(\frac{\cos\sqrt{\lambda}}{\sin\sqrt{\lambda}}\cos\sqrt{\lambda}y - \sin\sqrt{\lambda}y\right) \tag{74}$$

Solution (70) with P, V as above describes standing waves in the granular gas. The result is clearly not valid at resonance frequencies $\sqrt{\lambda} = n\pi$ that corresponds to the characteristic frequencies

$$\omega_r = \sqrt{\pi n \frac{k_s*}{H^2 P(\alpha_{sa})\left(\alpha_{s\psi}^{1/3} - \alpha_{sa}^{1/3}\right)}} \tag{75}$$

where n is an integer. One might argue that the singularity in the amplitude is in practice eliminated by dissipation effects, such as particulate viscosity. The situation may turn out to be quite similar to that of resonance tubes (see Ref. Goldshtein et al., 1996 and the papers cited therein), where in a narrow frequency band around each resonant frequency, shock waves appear in a gas traveling to and fro in the tube being repeatedly reflected from the piston and from the closed end. The resonance oscillations in the vibro- and gas-fluidized beds merit an independent thorough investigation.

In the region $\alpha_{sa} > \alpha_{s\psi}$ one has $\lambda<0$, and the solution of the problem is

$$V(y) = \frac{e^{\sqrt{-\lambda}}}{e^{\sqrt{-\lambda}} - e^{-\sqrt{-\lambda}}}e^{\sqrt{-\lambda}y} - \frac{1}{e^{2\sqrt{-\lambda}} - 1}e^{-\sqrt{-\lambda}y}$$

$$\Phi(y) = -\frac{\alpha_{sa}\sqrt{-\lambda}}{\delta}\left(\frac{e^{\sqrt{-\lambda}}}{e^{\sqrt{-\lambda}} - e^{-\sqrt{-\lambda}}}e^{\sqrt{-\lambda}y} + \frac{1}{e^{2\sqrt{-\lambda}} - 1}e^{-\sqrt{-\lambda}y}\right) \tag{76}$$

As one could anticipate no resonant frequencies exist in this case.

The above analysis shows that small vibrations of the upper plate result in unsteady flow patterns where the particle velocity and volume fraction oscillate about the stationary solution. Such flow patterns take place irrespectively of the fact whether the fully disperse fluidized bed is stable as in the case $\alpha_{sa}<\alpha_{s\psi}$ or unstable as in the case $\alpha_{sa} > \alpha_{s\psi}$. Forced vibrations of the upper plate prevent evolving of the instability described in Section 5. Perturbations of the velocity and particle fraction change now periodically in the form prescribed by Eq. (70). One can anticipate that the small vibrations will stabilize the disperse fluidized bed with decreasing volume fraction as well.

We discuss now the effect of vibrations on the flow patterns where the inverted packed bed (plug) is formed. Recall that such flow patterns can appear when the dimensionless group Π_g takes on sufficiently large values.

The influence of low-frequency vibrations upon layers of solid particles was thoroughly

investigated by Goldshtein et al. (1995) in regimes where the effect of air flow is negligible. They revealed that with increasing frequency ω the layers detach from the vibrating plate and pass through three vibrational states, with the respective behaviors being as of a solid plastic body, a liquid, and a gas. In the gas-like state the collisional character of particle motion is most obvious, the compression and expansion waves propagate along the layer. These results imply that the inverted packed beds can possibly be affected by vibrations of the upper plate in order to bring it to fluidization. Then, the combined effect of vibrations and gas flowing from below leads to a fluidization regime, which is also a subject of current and future investigations (Fichman et al., 1995; Goldshtein et al., 1999).

7. Conclusions

The present paper considers fluidization of gas–solid systems in confined volumes (tubes). We describe two possible fluidization regimes, namely a disperse fluidized bed and a plug adjacent to the upper distribution plate. Realization of these regimes is governed by the constitutive dimensionless parameters, in particular, that connected with gravity (see Eq. (44)), dimensionless fluidization velocity, and the ratio of the bed and tube heights. Existence of the disperse regime had not been hitherto reported in the literature. These regimes are modeled theoretically using one-dimensional gas-particle flow equations combined with the Goldshtik's model for the particle kinetic energy production. An experimental verification of the existence of the disperse regime has been performed. The theoretical study includes also an analysis of stability of stationary disperse fluidized beds and combined vibro- and gas-fluidized beds. The latter contemplates a new area in applied research on fluidization.

Acknowledgements

This research was supported by the Fund for the Promotion of Research at the Technion. The authors are grateful to Dr. B. Skacheck for help in performing calculations of particles' volume fraction distribution for several fluidization regimes.

Appendix A. Calculation of particle fraction distribution within the confined volume

Define the following integral function

$$I(y) = \int_{-1}^{y} \alpha_s(y)\, dy \tag{A1}$$

Then, the integration of differential equation (45) under the integral condition (49) may be reduced to solving the following system of two differential equations

$$\frac{d\zeta}{dy} = -11.17 \Pi_g \frac{K(\zeta)}{\zeta - \zeta_\psi} \zeta^3,$$

$$\frac{dI}{dy} = \zeta^3,$$

$$\zeta = \zeta_0, \quad I = 0 \quad \text{at} \quad y = -1$$

$$I(0) = 0.63 H_p/H = \alpha_{sa} = \zeta_{sa}^3 \tag{A2}$$

with $\zeta_\psi = 0.684$. The last condition imposed on $I(0)$, stemming from Eq. (49), enables one to determine the yet unknown parameter ζ_0.

This problem may be solved by the method of shooting. In particular, if $\zeta_{sa} < \zeta_\psi$, the required value ζ_0 lies necessarily in the region $0 < \zeta_0 < \zeta_\psi$. On the other hand, if $\zeta_\psi > \zeta_{sa}$ then ζ_0 lies in the region $\zeta_\psi < \zeta_0 < \bar{\zeta} = 0.63$.

As an example, we consider

$$\rho_g^0/\rho_s^0 = 10^{-3}, \quad a = 2.5 \text{ mm}, \quad e = 0.94, \quad v_0 = 12 \text{ m/s}. \tag{A3}$$

Then, from Eqs. (38) and (44) one has

$$\Pi_g = 1.51, \quad U_0 = 1.04. \tag{A4}$$

Under such conditions the problem (A2) has a mathematical solution shown in Fig. A1 (curve 1). This solution where $\zeta_0 = 0.33$ corresponds to a shallow bed with the particle mass $H_p/H = 0.13$. It can be easily seen that this solution is physical only when $H \geq = 38$ mm, in which case the thickness H_p corresponds to one monolayer of spheres. Clearly, that condition $\zeta_0 = 0.37$ corresponds to still smaller values of H_p/H. A situation where $\zeta_0 = 0.37$ is shown in

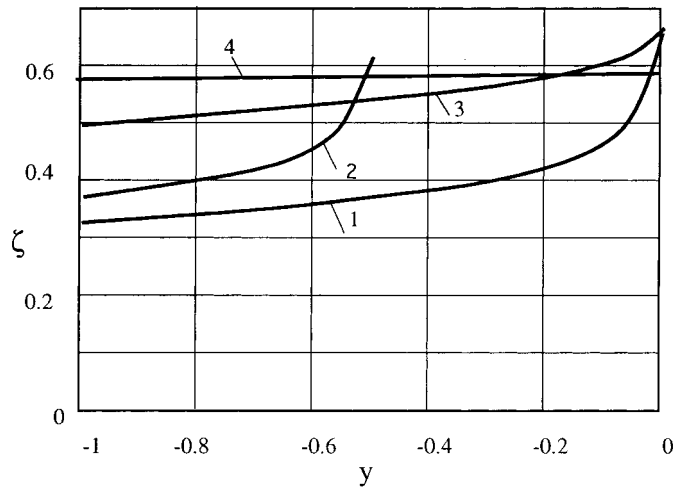

Fig. A1. Modified particle volume fraction ζ as function of the spatial coordinate y, $a = 2.5$ mm, $e = 0.94$. 1 — $\Pi_g = 1.51$, $U_0 = 1.04$, $H_p/H = 0.13$, $\zeta_0 = 0.33$, the solution has physical sense for beds with height $H = 38$ mm. 2 — $\Pi_g = 1.51$, $U_0 = 1.04$, $\zeta_0 = 0.37$, nonphysical solution since ζ reaches ζ_ψ within the bed. 3 — $\Pi_g = 0.1$, $U_0 = 1.04$, $H_p/H = 0.33$, $\zeta_0 = 0.5$. 4 — $\Pi_g = 0.01$, $U_0 = 1.04$, $H_p/H = 0.33$, $\zeta_0 = 0.57$.

Fig. A1, curve 2. The function ζ representing a particle volume fraction decreases with y reaching ζ_ψ within the bed at $y_{max} = -0.5$. As explained in Section 4, this is physically nonplausible. Thus, no physical solution exists in the example (A3) and (A4) of flow parameters.

The solutions corresponding to $H_p/H = 1/3$, $U_0 = 1.04$ and $\Pi_g = 0.1$ and $\Pi_g = 0.01$ are shown in Fig. A1 (curves 3 and 4, respectively). Note that in Fig. A1 (curve 3) the modified particle volume fraction ζ at the upper plate reaches the value ζ_ψ. On the other hand in the case shown in Fig. A1 (curve 4) at the upper plate one has $\zeta < \zeta_\psi$. In the latter case the disperse fluidized bed in the confined volume is almost homogeneous.

References

Batchelor, G.K., 1988. A new theory of the instability of a uniform fluidized bed. J. Fluid Mech. 193, 75–110.

Batchelor, G.K., Nitsche, J.M., 1994. Explosion of particles form a buoyant blob in a fluidized bed. J. Fluid Mech. 278, 63–81.

Buyevich, Yu.A., 1994. Fluid dynamics of coarse dispersions. Chem. Eng. Science 49 (8), 1217–1228.

Buyevich, Yu.A., Kapbasov, Sh.K., 1994. Random fluctuations in a fluidized bed. Chem. Eng. Science 49 (8), 1229–1243.

Buyevich, Yu.A., 1997. Particulate pressure in monodisperse fluidized beds. Chem. Eng. Science 52 (1), 123–140.

Fichman, M., Goldshtein, A., Gutfinger, C., Moldavsky, L., Pnueli, D., Shapiro, M., 1995. Method and apparatus for combined fluid vibrofluidized bed. (A superfluidized bed method and apparatus). Israeli patent No. 112687.

Ganser, G.H., Drew, D.A., 1990. Nonlinear stability analysis of a uniformly fluidized bed. Int. J. Multiphase Flow 16, 447–460.

Gidaspow, D., 1994. Multiphase Flow and Fluidization, Continuum and Kinetic Theory Description. Academic Press, Boston.

Gidaspow, D., Huilin, Lu., 1996. Collisional viscosity of FCC particles in a CFB. AICh Journal 42 (9), 2503–2510.

Glicksman, L.R., Hyre, M.R., Farrell, P.A., 1994. Dynamic similarity in fluidization. Int. J. Multiphase Flow 20, 331–386.

Goldshtein, A., Shapiro, M., 1995. Mechanics of collisional motion of granular materials. Part 1: General hydrodynamic equations. J. Fluid Mech. 282, 75–114.

Goldshtein, A., Shapiro, M., Moldavsky, L., Fichman, M., 1995. Mechanics of collisional motion of granular materials. Part 2: Wave propagation through vibrofluidized granular layers. J. Fluid Mech. 287, 349–382.

Goldshtein, A., Vainshtein, P., Fichman, M., Gutfinger, C., 1996. Resonance gas oscillations in closed tubes. J. Fluid Mech. 322, 147–163.

Goldshtein, A., Fichman, M., Gutfinger, C., Moldavsky, L., Pnueli, D., Shapiro, M., 1999. Investigation of vibrofluidization regimes in superfluidized beds, in preparation.

Goldshtik, M.A., Sorokin, V.N., 1968. Particle motion in vortex chamber. Zh. Prikl Mekh. Tekn. Fiz. (in Russian) 6, 17–25.

Goldshtik, M.A., 1972. Elementary theory of a fluidized bed. Zh. Prikl. Mekh. Tekhn. Fiz. (in Russian) 6, 106–112.

Goldshtik, M.A., Kozlov, B.N. 1973. Elementary theory of dense disperse systems. Zh. Prikl. Mekh. Tekn. Fiz. (in Russian) 4, 67–77.

Harris, S.E., Crighton, D.G., 1994. Solutions, solitary waves and voidage disturbance in gas fluidized beds. J. Fluid Mech. 266, 243–276.

Hirschfelder, J.O., Curtis, Ch.F., Bird, R.B., 1954. Molecular Theory of Gases and Liquids. Wiley, New York.

Koch, D.L., 1990. Kinetic theory for a nondisperse gas–solid suspension. Phys. Fluids A2 (10), 1711–1723.

Kuini, D., Levenspiel, O., 1991. Fluidization Engineering, 2nd ed. Butterworths, London.

Lammers, J.H.G., Biesheuvel, A., 1996. Concentration waves and the instability of bubbly flows. J. Fluid Mech. 328, 67–93.

Lim, K.S., Zhu, J.X., Grace, J.R., 1995. Hydrodynamics of gas–solid fluidization. Int. J. Multiphase Flow 21, 141–193.

Lun, C.K.K., Savage, S.B., 1987. A simple kinetic theory for granular flow of rough, inelastic, spherical particles. Trans. ASME: J. Appl. Mech. 54, 47–53.

Lun, C.K.K., Lin, H.S., 1997. Numerical simulation of dilute turbulent gas–solid flows in horizontal channels. Int. J. Multiphase Flow 23, 575–605.

Nigmatulin, R.I., 1978. Fundamentals of Mechanics of Heterogeneous Media (in Russian). Nauka, Moscow.

Jackson, R., 1963. The mechanics of fluidized beds. I. The stability of the state of uniform fluidization. Trans. Inst. Chem. Engs. 41, 13–21.

Rubinow, S.I., Keller, J.B., 1961. The transverse force on a spinning sphere moving in a viscous fluid. J. Fluid Mech. 11, 447–459.

Yerushalmi, J., Cancurt, N.T., 1979. Further studies of the regimes of fluidization. Powder Technology 24, 187–205.

Wallis, G.B., 1969. One-Dimensional Two-Phase Flow. McGraw-Hill, New York.

Zenit, R., Hunt, M.L., Brennen, C.E., 1997. Collisional particle pressure measurements in solid–liquid flows. J. Fluid Mech. 353, 261–283.